

Article

# Climatically-Controlled River Terraces in Eastern Australia

James S. Daley<sup>1,2,\*</sup>  and Tim J. Cohen<sup>3,4</sup><sup>1</sup> Griffith Centre for Coastal Management, Griffith University, Gold Coast, QLD 4215, Australia<sup>2</sup> School of Earth and Environmental Science, University of Queensland, St. Lucia, QLD 4072, Australia<sup>3</sup> ARC Centre of Excellence for Australian Biodiversity and Heritage–School of Earth and Environmental Sciences, University of Wollongong, Wollongong, NSW 2522, Australia; tcohen@uow.edu.au<sup>4</sup> GeoQuEST Research Centre–School of Earth and Environmental Sciences, University of Wollongong, Wollongong, NSW 2522, Australia

\* Correspondence: j.daley@griffith.edu.au

Academic Editors: Jef Vandenberghe, David Bridgland and Xianyan Wang

Received: 23 August 2018; Accepted: 13 October 2018; Published: 16 October 2018



**Abstract:** In the tectonically stable rivers of eastern Australia, changes in response to sediment supply and flow regime are likely driven by both regional climatic (allogenic) factors and intrinsic (autogenic) geomorphic controls. Contentious debate has ensued as to which is the dominant factor in the evolution of valley floors and the formation of late Quaternary terraces preserved along many coastal streams. Preliminary chronostratigraphic data from river terraces along four streams in subtropical Southeast Queensland (SEQ), Australia, indicate regionally synchronous terrace abandonment between 7.5–10.8 ka. All optically stimulated luminescence ages are within 1 $\sigma$  error and yield a mean age of incision at  $9.24 \pm 0.93$  ka. Limited samples of the upper parts of the inset floodplains from three of the four streams yield near-surface ages of 600–500 years. Terrace sediments consist of vertically accreted fine sandy silts to cohesive clays, while top stratum of the floodplains are comprised of clay loams to fine-medium sands. The inundation frequency of these alluvial surfaces depends on their specific valley setting. In narrow valley settings, where floodplains comprise <5% of the valley floor, terraces are inundated between the 20 and 50-year annual exceedance probability (AEP) flood, while in wide settings (floodplains >20%), the terraces are no longer inundated. Floodplain inundation frequencies also vary between these settings by an order of magnitude between 5- to 50-year AEP, respectively. The correlation of terrace abandonment within SEQ with fluvial and palaeoenvironmental records elsewhere in the subtropics, and more broadly across eastern Australia, are an indication that terrace abandonment has primarily been driven by climatic forcing. Contemporaneous channel incision in the early Holocene may have been driven by an increasingly warmer and wetter environment in SEQ, with a climate commensurate with the delivery of more extreme weather events. Following channel incision, many streams in SEQ have been largely confined to their entrenched “macrochannel” form that remains preserved within the valley floor.

**Keywords:** terrace; channel entrenchment; extrinsic controls; Holocene; climate; optically stimulated luminescence; OSL; eastern Australia

## 1. Introduction

River terraces typically form due to tectonic or climatic controls but can also develop due to intrinsic factors (within-system changes, such as slope threshold exceedance, channel avulsion, or stream capture) [1–3], as well as direct or indirect human disturbances [4,5]. In tectonically-controlled settings, persistent uplift can create terrace staircases several hundred of meters above the present

channel, preserved over millennia [6,7]. However, even in such settings, climatic controls can remain critical factors that cause subsequent incision [8]. A global comparison of terrace sequences reveals that terrace formation is dominantly a climatically-induced process, commonly associated with transitions between glacial and interglacial cycles. Issues remain regarding the exact timing of terrace development within the climatic cycle, which may depend on other geoclimatic factors [9–13]. Generally, aggradation is initiated during glacial cycles and pronounced channel incision occurs during the subsequent deglacial (warming) phase. Channel incision and floodplain abandonment (e.g., Figure 1) may reflect changes in discharge or sediment regimes associated with rainfall, vegetation changes, or weathering/erosion production [13].

In Australia, low to negligible rates of tectonic uplift and denudation over the past ca. 30 Ma [14,15], along with high streamflow variability [16,17], ensure terraces are abandoned relatively slowly. Shallow alluvium in narrow valley settings often feature polycyclic alluvial units which are only partially removed under subsequent climatic regimes [18,19]. In southeastern Australia, debate has ensued as to whether terraces have formed in response to climatic controls or intrinsic properties [20,21]. In this region, chronological investigation of alluvial fills has identified a hiatus in sedimentary records from ca. 10–4.5 ka [21,22]. This gap was initially interpreted as an erosional void caused by episodic but laterally active river systems under a warmer and wetter climate, termed the Nambucca Phase and comparative in timing to the Holocene hypsithermal [22]. Contemporaneous terrace abandonment and erosion occurred in two basins on the subtropical eastern seaboard Nambucca and Bellinger basins [18,22] (Figure 2B) and a comparative alluvial gap has also been identified in the wet tropics [23–25].

Additional palaeoclimatic records (e.g., pollen, charcoal, and other biological indicators) suggest increased warming or precipitation between 10–6 ka in eastern Australia [26–29] accompanied by abrupt changes in vegetation cover, with a significant expansion of arboreal taxa recorded from 10 ka [30–32]. Increasing lake levels (relative to today) across the continent provide further indication of a broad increase in effective precipitation [33–35]. In the eastern highlands, wet conditions for peat formation occurred from ca. 9–6 ka [36] and a reduction in charcoal abundance on the subtropical North Stradbroke Island also indicates regionally wetter conditions at this time [31]. A general reduction in rainfall has been interpreted from ca. 6 ka [28,37].

In contrast, geomorphic responses to intrinsic drivers can produce a range of chronologically disjunct terraces along a channel network [18]. Indeed, upstream channel instability can result in downstream infilling and apparent asynchronicity in longitudinal and adjacent valley fills [38]. A focus on catastrophic floodplain formation and pseudo-cyclic river behavior has emerged from the Australian geomorphic literature [39–41]. The role of large floods has been implicit in the understanding of past and present river dynamics and form-process relationships in southeastern Australia [39–42]. Large-magnitude flood events often act as geomorphic perturbations that exceed thresholds of channel stability and adjust the channel boundaries [42,43]. As such, intrinsic factors such as within-channel sedimentation, channel avulsion, and stochastic events have been suggested as the dominant mechanism in the dynamic evolution of late Quaternary alluvial units in eastern Australia [20,41].

Research in Southeast Queensland (SEQ) has highlighted that the riverine response to extensive high-magnitude flooding in recent years was largely affected by the presence of entrenched river channels, termed macrochannels [44–49]. Macrochannels were first described in the South African Sabie River [50,51], but similar channel forms have been identified elsewhere [52–54]. Such streams feature large, compound river channels where multiple alluvial units are inset within a broader, entrenched channel (Figure 1). An active low-flow channel lies within this much larger “macrochannel”, which can accommodate flood waters of extreme magnitude. Along Lockyer Creek in SEQ, synchronous incision of a Pleistocene terrace after 11.5–9.3 ka suggests the macrochannel formed rapidly as a basin-wide response [46]. However, given the extent of these findings are limited to the partly-confined, mid-reaches of Lockyer Creek, it remains unclear whether channel entrenchment and terrace abandonment was a single-basin phenomenon or reflects a regional scale response.

This is a critical question with regard to understanding regional stream patterns and the inherent drivers of macrochannel formation. Regional integration of fluvial processes, such as channel entrenchment, can provide substantial evidence of the factors driving channel change [11,55]. Did channel entrenchment in SEQ occur coevally or have intrinsic factors driven an asynchronous response? This paper investigates adjacent alluvial units at four sites throughout SEQ exhibiting macrochannel morphologies to determine the chronological characteristics of the channel boundary and whether Quaternary regional climate change has had an impact on contemporary river systems.



**Figure 1.** Field photo from the left bank of the incised Lockyer Creek macrochannel, exhibiting inset benches, steep banks, and a terrace surface beyond the macrochannel boundary. Bankfull capacity of the macrochannel exceeds the 50-year recurrence interval.

## 2. Materials and Methods

### 2.1. Site Selection and Fieldwork

SEQ is a biogeographical region ranging in latitude from 26° to 28° south, along the central eastern coast of Australia (Figure 2), consisting of four coastal basins with a total area of approximately 20,400 km<sup>2</sup> that rise along the eastern slopes of the Great Dividing Range. The region includes the major metropolitan areas of Brisbane and the Gold Coast (Figure 2). The geology of SEQ has primarily developed from a complex series of tectonic processes from the Late Palaeozoic onwards, primarily associated with the development of the New England Orogen. The dominant lithologies are broadly comprised of Palaeozoic to early Triassic metasediments, Mesozoic intracratonic sedimentary basins and intrusive granites, and early Miocene volcanics capping the highland regions along the basin boundaries (Table 1). Erosion-resistant Palaeozoic metamorphic and igneous lithologies dominate much of the highlands throughout the region while the lowland and coastal regions are mostly comprised of Mesozoic sedimentary basins and more recently deposited sediments.

The SEQ region has a subtropical climate with mean monthly temperatures between 21 to 29 °C and annual rainfall between 700–2200 mm. High seasonal, inter-annual and inter-decadal variability in rainfall is driven by a number of Pacific climate phenomena that modulate ocean temperatures, pressure gradients, and precipitation across the Indo-Pacific region, including the El Niño-Southern Oscillation (ENSO) and the Inter-Decadal Pacific Oscillation (IPO) [56–59]. Most rainfall occurs in the summer months between October and February followed by a relatively dry winter. The most

substantial sources of precipitation for the region are summer-dominated, east-coast, low-pressure systems and the southward migration of post-tropical cyclone storms.

Extreme climatic events are frequent and include long-term droughts, very intense rainfall, flooding, and flash flooding. Significant localized variations in annual rainfall are also driven by orographic effects related to the presence of highland ranges along basin divides. SEQ is broadly characterized by a high index of flood variability, particularly in the major river systems. A review of flood variability along the east coast of Australia found from three metrics that peak discharge variability occurs in SEQ, declining to the south in the relatively smaller Gold Coast streams [17].

Four study sites within SEQ were selected for geomorphic and chronostratigraphic analysis, including the Brisbane, Logan, and Albert Rivers and Lockyer Creek (Figure 2). Study sites were paired with stream gauging stations (with minimum record lengths of 58 years) to provide an association of alluvial surfaces with contemporary inundation frequencies. Flood frequency analyses utilized the Generalised Extreme Value of the annual maximum series for water years (September–August) and is further detailed in [60]. All sites are located in the mid-reaches of their valleys and feature macrochannel morphologies with varying degrees of inset alluvial units, but all are characterized as having Quaternary alluvium on both channel margins.

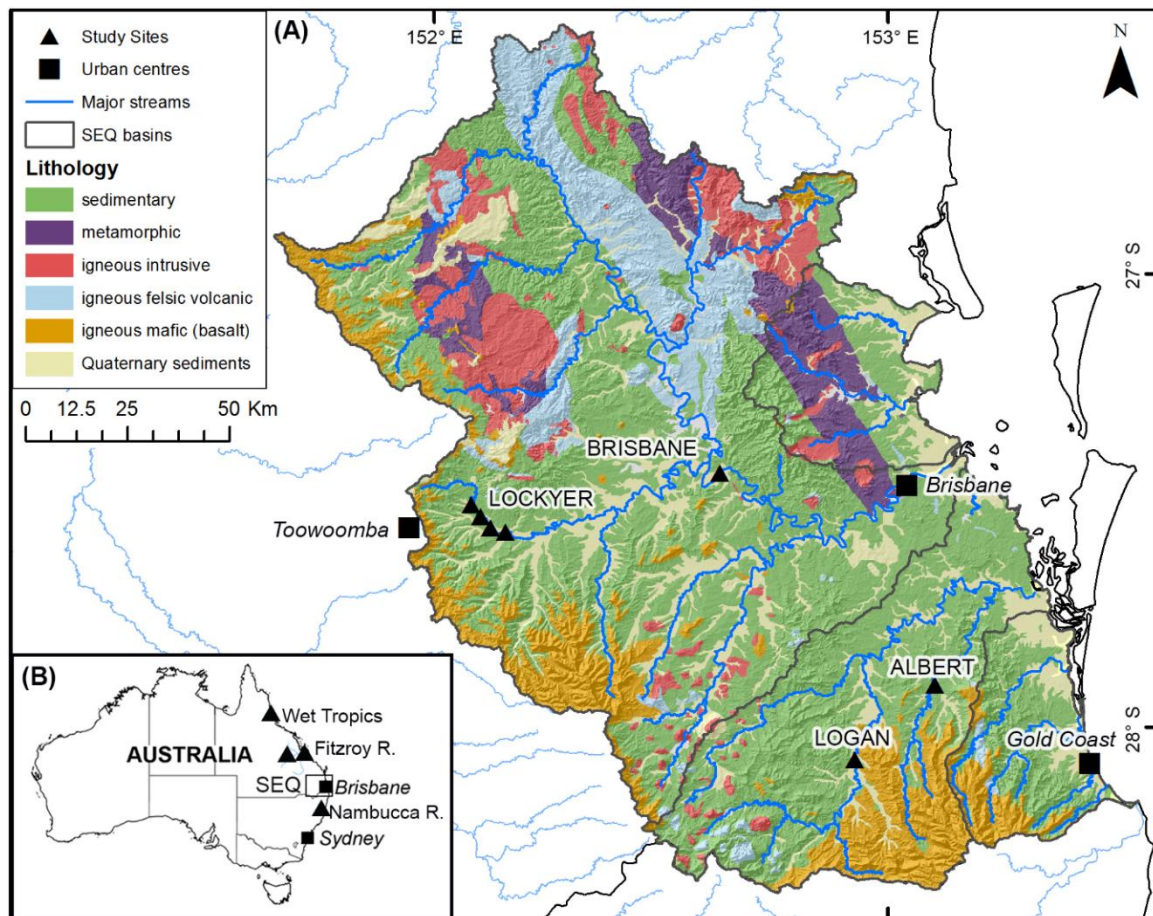


**Figure 2.** (A) Location map of study sites, major streams, and basins in SEQ, Australia. Underlying base map shows 1:1M Surface Geology (Geoscience Australia) (B) Inset shows the location of SEQ in Australia and additional site locations discussed in text.

Geomorphic mapping was undertaken by delineating units through hypsographic analysis, using a probability distribution function, of a detrended digital elevation model (DEM), derived from 1 m LiDAR data [61,62]. Alluvial valley floors were identified as relatively flat-lying (<2° slope) surfaces adjacent to the channels. Based on the presumption that alluvial units are generally flat-lying, breaks

in the slope of the curve define the boundaries between adjacent landforms, which were classified based on their relative height above the channel. Peaks in the hypsographic curve are indicative of a higher proportion of the valley floor associated with a given elevation range. Breakpoints were assessed against slope class intervals and hillshade rasters derived from the DEM for consistency with user-identified geomorphic breaks.

Field observations were undertaken to characterize the geomorphic structure (Figure 1) and verify mapping at each site. Near-surface sediments on the adjacent terrace and inset units were targeted for geochronology to determine how recently surface sediments that form the macrochannel boundaries were deposited. The terraces are presumed to be fill terraces following chronostratigraphic descriptions in the Lockyer Creek basin [46]. In some circumstances, the Lockyer Creek terrace sits on an elevated bedrock strath surface, but preservation of older basal material within inset units suggests the underlying bedrock strath existed prior to the deposition of the alluvial fill [46]. However, as only short cores were collected in this study, the alluvial units investigated in this study are presumed to be equivalent to those of Lockyer Creek given the proximity of the sites and comparative forms of the valley floors.

The sampling approach assumed that ages from terrace surfaces reflected the last period of valley floor aggradation, vis-à-vis abandonment. Bank exposures were analyzed at two sites, and short cores up to 3 m long were extracted in units directly adjacent to channel banks using a hand-held percussion corer to date the abandonment age of various alluvial surfaces.

**Table 1.** Summary details of field sites.

| Site Location                    | Lockyer Creek                                                                                                                                        | Logan River                                                                                                                            | Albert River                                                                                                                           | Brisbane River                                                                                                                                                                                  |
|----------------------------------|------------------------------------------------------------------------------------------------------------------------------------------------------|----------------------------------------------------------------------------------------------------------------------------------------|----------------------------------------------------------------------------------------------------------------------------------------|-------------------------------------------------------------------------------------------------------------------------------------------------------------------------------------------------|
| Gauge ID                         | 143203                                                                                                                                               | 145008                                                                                                                                 | 145102                                                                                                                                 | 143001                                                                                                                                                                                          |
| Gauge Name                       | Helidon                                                                                                                                              | Round Mountain                                                                                                                         | Bromfleet                                                                                                                              | Vernor                                                                                                                                                                                          |
| Drainage area (km <sup>2</sup> ) | 357                                                                                                                                                  | 1262                                                                                                                                   | 544                                                                                                                                    | 10,172                                                                                                                                                                                          |
| Distance upstream (km)           | 99                                                                                                                                                   | 125                                                                                                                                    | 47                                                                                                                                     | 131                                                                                                                                                                                             |
| Elevation (m)                    | 129                                                                                                                                                  | 44                                                                                                                                     | 28                                                                                                                                     | 18                                                                                                                                                                                              |
| Slope (m·m <sup>-1</sup> )       | 0.002                                                                                                                                                | 0.001                                                                                                                                  | 0.001                                                                                                                                  | 0.0002                                                                                                                                                                                          |
| Stream order                     | 6                                                                                                                                                    | 6                                                                                                                                      | 6                                                                                                                                      | 8                                                                                                                                                                                               |
| Channel setting                  | partly confined                                                                                                                                      | partly confined                                                                                                                        | partly confined                                                                                                                        | partly confined–unconfined                                                                                                                                                                      |
| Bankfull AEP (a <sup>-1</sup> )  | >200                                                                                                                                                 | 20                                                                                                                                     | 40                                                                                                                                     | 48                                                                                                                                                                                              |
| Bed load                         | mixed sand-cobble                                                                                                                                    | m/c sand                                                                                                                               | m/c sand                                                                                                                               | mixed sand–cobble                                                                                                                                                                               |
| Primary geology <sup>1</sup>     | Lithofeldspathic labile and feldspathic labile sandstone; quartzose sandstone, siltstone, shale, minor coal, ferruginous oolite marker               | Lithofeldspathic labile and feldspathic labile sandstone; quartzose sandstone, siltstone, shale, minor coal, ferruginous oolite marker | Lithofeldspathic labile and feldspathic labile sandstone; quartzose sandstone, siltstone, shale, minor coal, ferruginous oolite marker | Lithofeldspathic labile and feldspathic labile sandstone                                                                                                                                        |
| Secondary geology <sup>1</sup>   | Quartz-lithic and quartzose sandstone, quartz-rich granule conglomerate, silty sandstone, siltstone, claystone; carbonaceous siltstone and claystone | Alkali-olivine basalt                                                                                                                  | Alkali-olivine basalt                                                                                                                  | Feldspathic and lithic meta-arenite, metasiltstone and conglomerate proximal turbidites, with structurally intercalated or stratigraphically underlying chert, jasper and basic meta-volcanics. |
| Soils <sup>2</sup>               | Fine textured alluvium—hardsetting brown and grey loam surface soil over neutral to alkaline clay                                                    | Fine textured alluvium—black earth and grey clays                                                                                      | Fine textured alluvium—black earth and grey clays                                                                                      | Fine textured alluvium—black earth and grey clays                                                                                                                                               |

<sup>1</sup> Geological descriptions after 1:25,000 scale Geoscience Data, Queensland Mapping Data. <sup>2</sup> Soil descriptions after 1:2,000,000 scale Digital Atlas of Australian Soils.

## 2.2. Chronology

Cores were examined under subdued red-light (>590 nm) conditions and sampled for luminescence and particle size analysis. Grain size was described from field texture tests using grain size class intervals [58], to primarily distinguish between clay, loam, sand, and gravels. Particle size analysis using a Mastersizer (Malvern Instruments, Malvern, UK) was undertaken on representative samples to verify field textures and the relative change with depth. The degree of alteration or pedogenesis (e.g., iron staining, carbonates, or ped development) was described based on the presence of sedimentary structures and the nature of contact between unit boundaries.

A combination of optically stimulated luminescence (OSL) and radiocarbon dating was used to establish the chronology of the sites across the four rivers. In total, nine samples were analyzed for OSL analysis and two charcoal samples were analyzed for radiocarbon determinations. OSL samples were collected from the center of cores with particular care to avoid stratigraphic boundaries following standard procedures by [63,64]. Following the pre-treatment of samples to remove carbonates, organics, feldspars, and heavy minerals, single-grain (180–220  $\mu\text{m}$ ) quartz sands were etched in 48% hydrofluoric acid for 40 min to remove the outer 10  $\mu\text{m}$   $\alpha$ -irradiated rind. Etched grains were analyzed using optical stimulation, and equivalent dose ( $D_e$ ) values on individual grains were determined according to the modified single aliquot-regenerative dose (SAR) protocol [65] and Risø instrumentation described therein, using the acceptance criteria listed by [66]. Age modelling from measured  $D_e$  values followed the well-established approach of [67–70]. Equivalent dose determination of two samples with high overdispersion ( $\sigma_d$ ) followed [66] by fitting a single Gaussian curve to the peak of a multi-Gaussian summed probability distribution. The final age determinations are summarized in Table 2.

Lithogenic radionuclide concentrations were analyzed from sediments adjacent to OSL samples using high-resolution gamma spectrometry for  $^{238}\text{U}$ ,  $^{226}\text{Ra}$ ,  $^{210}\text{Pb}$ ,  $^{232}\text{Th}$ , and  $^{40}\text{K}$  concentrations [71]. Dose rates were calculated using the conversion factors [72] and  $\beta$ -attenuation factors [73]. Cosmic dose rates were calculated from [74] using an alpha-efficiency “ $\alpha$ ” value of  $0.04 \pm 0.02$  [75]. Water content was measured directly from each sample and assigned errors of  $\pm 5\%$  to account for uncertainty. Water content was assumed to be representative of saturation levels over the full period of burial.

Radiocarbon analyses on charcoal fragments were conducted at Beta Analytic Inc. laboratory using the  $^{14}\text{C}$  Accelerator Mass Spectrometry (AMS) technique, with age and error calculations following parameters outlined by [76]. Table 3 presents radiocarbon results as conventional  $^{14}\text{C}$  ages and calibrated ages in cal. ka BP using the SHCAL13 database [77].

## 3. Results

### 3.1. Integrity of Chronology

Chronological data for OSL samples is presented in Table 2 and for radiocarbon in Table 3. All eight OSL samples exhibited good luminescence characteristics. Optical ages were all from single-grain determinations. For samples 16-0115-002, 16-0115-005, 16-0115-007, 16-0115-008, and 16-0115-009,  $D_e$ s were calculated using the central age model (CAM) [69]. The low  $\sigma_d$  values in the range of 15–20% suggested complete bleaching and hence the use of the CAM (Figure 3A). For sample 16-0115-001, although the  $\sigma_d$  was 28%, no clear stratigraphic distinction could be made between this and the underlying sample (with a lower  $\sigma_d$ , sample 16-0115-002; Table 2). In this case, the CAM was accepted. Some samples had high  $\sigma_d$  (25–60%), and in these instances, age models were employed on a sample-by-sample basis.

In some examples, the difference between the  $D_e$  returned from the CAM and the minimum age model (MAM) had no impact on the final age determination, with the ages for each model within  $1\sigma$  error (sample 16-0115-004 in Table 2; the  $D_e$ s for both models are presented in Figure 3B). Sample 16-0115-0003 displayed a high degree of mixing and over-dispersion of 60%. For samples such as this (and 16-0115-004, Figure 2B), equivalent doses determined that using the MAM yields results were consistent with the dominant population of a finite mixture model (FMM) and the multi-Gaussian

summed probability approach. As such, the MAM was selected for these two samples and it was assumed they were partially bleached. However, the low-dose components identified in some of the samples were likely to be a contamination signal due to bioturbation (e.g., grain intrusion).

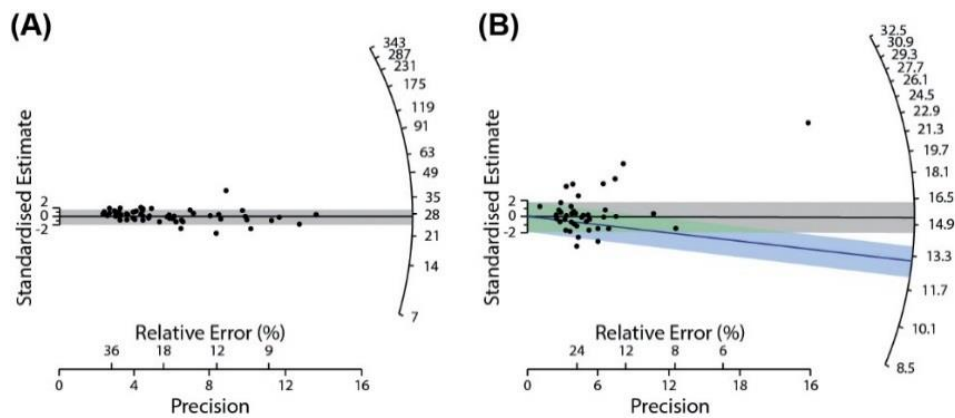


**Figure 3.** Radial plots for OSL samples displaying equivalent doses ( $D_e$ ) and model predictions for (A) 16-0115-0002, and (B) 16-0115-0004. The black line is CAM and the blue line is MAM.

### 3.2. Valley Floor Characteristics

Valley floors across the four sites were 0.5–3 km wide and were characterized by dissected floodplain surfaces in partly confined settings. The Logan and Albert Rivers had similar bed slopes of  $0.001 \text{ m}\cdot\text{m}^{-1}$  and basin areas varied between 540 and  $1260 \text{ km}^2$  (Table 1). All four study sites featured the same primary underlying geology (Table 1). Three of the four basins shared the same geological units in their upper basins, draining predominantly basalts and feldspathic sedimentary lithologies (Figure 2). The Brisbane River site was in the partly confined mid-reaches of the basin and was located several kilometers downstream of its junction with Lockyer Creek. The reach features the same underlying geology found in the mid- to lower Lockyer, but upstream it was dominated by metasediments (Table 1). The stream abruptly changed course at the downstream extent of the study reach as it again abutted this lithological unit (Figure 4A). The Brisbane reach had a slope of  $0.0002 \text{ m}\cdot\text{m}^{-1}$  and a basin area an order of magnitude larger than the other sites (Table 1). All streams featured comparative morphologies to the Lockyer Creek [46,49]. In all settings, infrequently inundated valley floors bound comparatively narrow macrochannels 50–100 m wide that featured an active channel and inset alluvial units, with up to four alluvial units across the valley floor; bars, benches/inset floodplains, and terraces. The channels were low-sinuosity, but featured sharp, structurally-controlled bends. However, two valley settings could be distinguished by the spatial extent of their floodplains.

Figure 4A shows the distribution of alluvial units along the Brisbane River at Vernor (mid-Brisbane). The wide floodplain setting was comparable to the Lockyer Creek at Helidon, where floodplain formation had been influenced by changes in variations in underlying lithology [46]. The valley floor on the Brisbane River had a complex morphology (Figure 4A). The site featured a number of alluvial units, with floodplains comprising 30–40% of the valley floor within the reach (Figure 4A). However, the floodplain had a recurrence interval for overtopping of 50 years under the current flow regime (annual maximum series), while the T1 terrace on the Brisbane River exceeded the 100-year recurrence interval flood and there were no records it had been inundated in historical records. In the mid-Brisbane reach, a higher terrace (T2 in Figure 4A) occurred as discontinuous remnants  $\approx 4 \text{ m}$  above the T1 terrace. However, it was unclear whether there were two terrace surfaces or whether the apparent height difference between the two terraces was simply a function of drainage development and terrace dissection. The T1 terrace and floodplain on the mid-Brisbane were heavily dissected, with numerous palaeochannels and meander cut-offs within inset units across the valley floor. While T2 was comparatively less dissected, it featured higher order drainage development along its margin with

T1 (Figure 4A). At this location, we have mapped the terraces as two separate units, but we do not have chronological or stratigraphic control that allowed us to verify this. This upper T2 terrace was also clearly identified along the Logan River, with similar drainage features (Figure 4C), but was not present along other streams and was not further investigated in this study.

In comparison to the Brisbane River, the valley floor morphology in the other locations was comparatively simple (Figure 4B). In these settings, the valley floor was dominated by a single terrace (T1) which occupied up to 90% of the valley floor. Floodplains were comparatively narrow (10–30 m wide) and are commonly referred to as alluvial benches within the Australian literature [40,78,79]. These were inset within the macrochannel and are inundated by 2–5-year annual exceedance probability (AEP) floods. Valley floors were up to 2 km wide and were dominated by the T1 terrace, which formed the boundary of the macrochannels, was longitudinally continuous down valley, and has inundation frequencies of between the 20 and the 50-year AEP. Occasional palaeochannels along T1 suggested comparative channel widths prior to abandonment (Figure 4B).

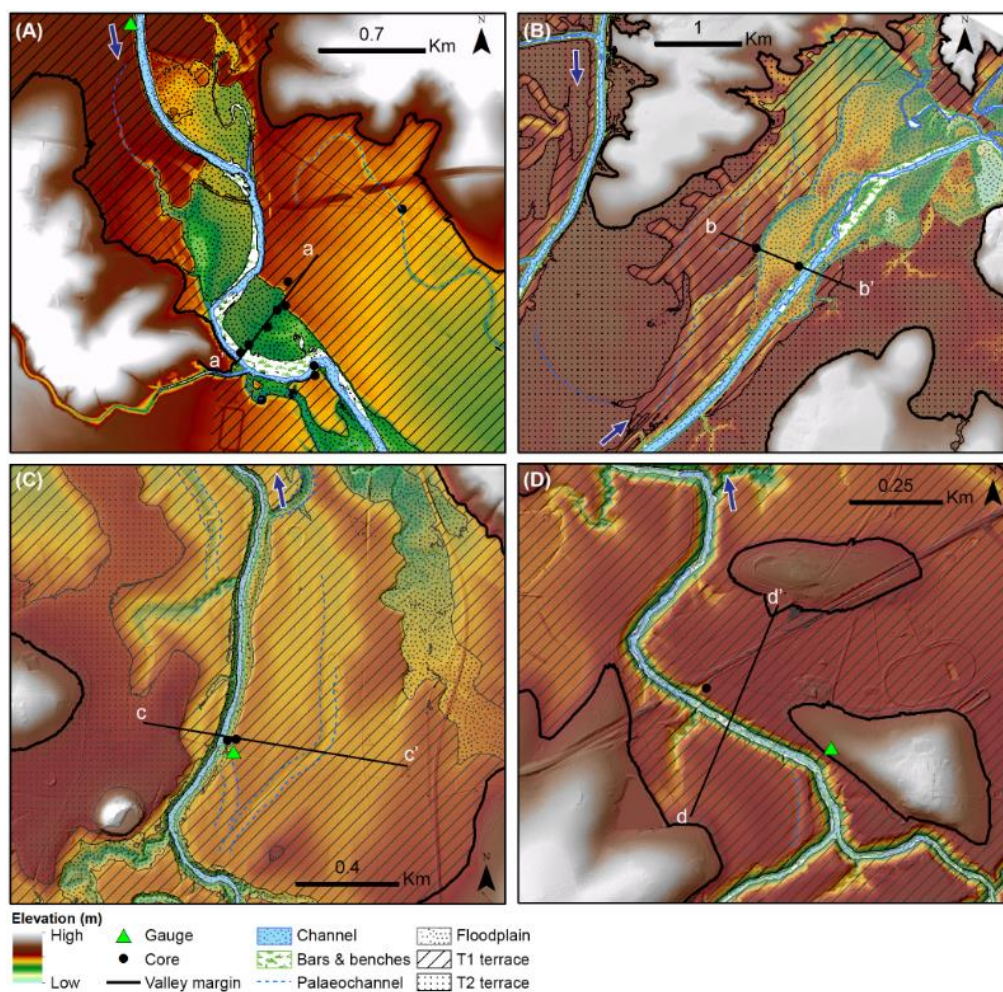


**Figure 4.** Representative geomorphic maps showing the distribution of alluvial units and the spatial extent of terraces along the valley floor for (A) Lockyer Creek at Site 3 (Helidon), (B) Brisbane River at Verner, (C) Logan River at Round Mountain, (D) Albert River at Bromfleet. Also shown are the location of cores, stream monitoring gauges, and valley cross sections shown in Figure 5. Blue arrows indicate flow direction. Gauge locations for Brisbane River are <500 m beyond the mapping extent of (B).

### 3.3. Alluvial Sedimentology and Chronology

Short cores 1–4 m in length were collected from units adjacent to the channel at each site (Figure 5). Terraces sediments were consistent with overbank vertical accretion and were comprised of fining up,



light brown, very fine–fine sandy silts, to a dense, black silty clay. Silt and clay content varied with depth, but was overall relatively homogenous. The stratigraphic relationships varied across sites, but overall expression of sediments was relatively consistent (Figure 5). At three sites, the upper facies of the terrace consisted of highly cohesive black clay (7.5 yr 2.5/1) and showed a gradual down-profile transition to sandier units. No mottling was apparent in the cores, but Fe concretions and detrital carbonates <2 mm diameter were present throughout the cores at 0.5–1.5 m depths.

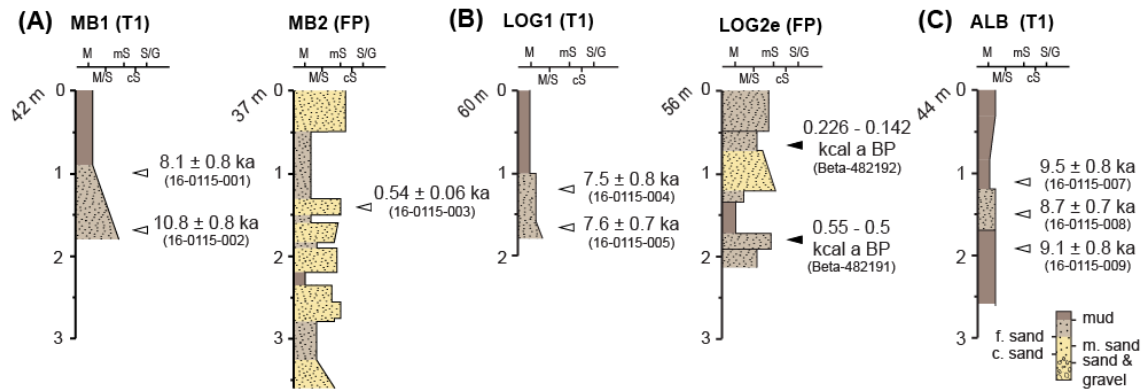


**Figure 5.** Core logs sedimentology and chronological data for (A) Brisbane River, (B) Logan River, and (C) Albert River. Geomorphic units are shown in brackets next to the log name; see Figures 1 and 4 for locality of sites and Figure 6 for transects.

Floodplain sediments were more stratigraphically variable and consisted of coarser-grained sediment than terraces, dominantly composed of unconsolidated clay loams to massive sands. The surficial units reflected overbank sediments on the floodplain levee comprised of vertically accreted, decimeter-thick beds. The loams consisted of light-brown to brown sandy clay loam to sandy clay with fine sands and small quantities of fragmented charcoal and minor ferruginous staining. Sharp boundaries occurred with massive beds of brown, fine–medium sand that featured increasing silt content down the profile. Sands were well sorted, unaltered, and had sharp contacts with adjacent units.

A preliminary terrace abandonment chronology was provided using OSL dating of near-surface sediments within terraces adjacent to terrace scarps within four basins, as well as basal floodplain material in Lockyer Creek (Table 2). OSL ages were obtained from 0.4–1.2 m to avoid soil disturbance associated with agriculture and have been used to infer the age of terrace abandonment. Sediments from the upper part of the T1 terrace along the mid-Brisbane River yielded age estimates ranging from  $8.08 \pm 0.77$  ka at 1.0 m and  $10.83 \pm 0.84$  ka at 1.7 m depth (Figure 6D). The ages were within  $2\sigma$  error of each other and had a mean age of  $9.46 \pm 0.90$  ka. While no basal ages were determined for the adjacent floodplain, a 0.4 m thick flood unit of fine sands in the floodplain levee returned a minimum age of  $0.54 \pm 0.06$  ka at 1.4 m depth (MB2, Table 2). Such deposition on this floodplain has been recorded anecdotally with recent flooding depositing a unit of massive sands at the surface 0.5 m thick. These chronological results from the Brisbane terrace site were comparable to what is observed in Lockyer Creek (Figure 6A,B), where nine OSL ages from the upper parts of the terraces, as well as basal ages from adjacent floodplains (Table 2), constrained the age of terrace abandonment to  $9.19 \pm 1.2$  ka (Figure 6).

Along the Logan River, sediments in the upper part of the T1 terrace have been dated at  $7.51 \pm 0.82$  ka (1.2 m; Figure 6D) and  $7.61 \pm 0.68$  ka (1.6 m; Figure 6D). The upper sample at 1.2 m yielded slightly older age estimates when a CAM was employed ( $8.88 \pm 0.81$  ka) but the estimates remained within  $1\sigma$  of the underlying sample, and as such, the age estimates from the MAM were used as the depositional age. In the adjacent inset floodplain, radiocarbon determinations on charcoal yielded calibrated ages of 226–142 cal. years BP at 0.65 m and 550–500 cal. years BP at 1.8 m (Table 3). Despite different methods of age determination, these much more recent ages compared with the age

of flood deposits in the inset floodplains along the Brisbane River and Lockyer Creek, although the present inundation frequency of these units differs by an order of magnitude (e.g., 5 year AEP at Logan River vs 50 year AEP at Brisbane River, Figure 6).

In the sediments along the Albert River, three terrace samples dated with OSL were all within error and indicated an age range of  $9.51 \pm 0.82$  ka,  $8.71 \pm 0.66$  ka, and  $9.08 \pm 0.81$  ka (1.1, 1.5, and 1.9 m respectively; Figure 6E). The ages yielded a mean pooled age of  $9.10 \pm 0.87$  ka, coeval with the age of abandonment in the Lockyer and Brisbane River (Figure 6C).

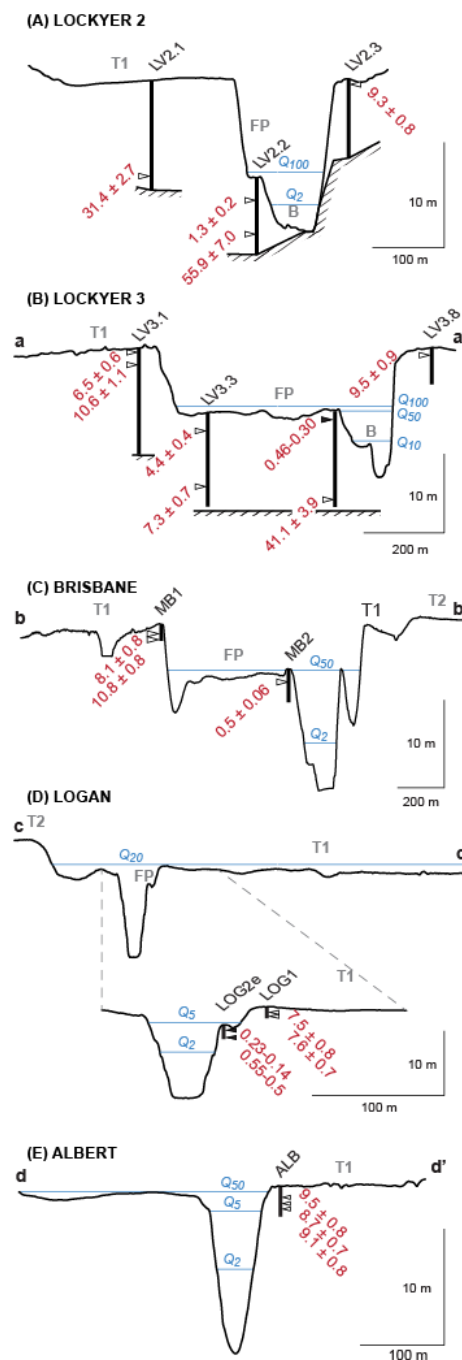


**Figure 6.** Representative valley cross sections and chronology for study sites (A) Lockyer Creek, Site 2, (B) Lockyer Creek, Site 3, (C) Brisbane River, (D) Logan River; and (E) Albert River. Location of cross sections are shown in planform in Figure 4. (A,B) Lockyer Creek sites and chronology after [46]. Flood frequency analyses and heights after [60].

**Table 2.** Summary of OSL data, description and ages ( $1\sigma$  errors). See Table S1 for complete OSL results.

| Basin           | Core ID | Lab Code    | Depth (m) | Landform   | Depositional Environment | Age (ka)         | Method |
|-----------------|---------|-------------|-----------|------------|--------------------------|------------------|--------|
| Mid-Brisbane    | MB1     | 16-0115-001 | 1.0       | Terrace    | Overbank                 | $8.08 \pm 0.77$  | CAM    |
|                 |         |             |           |            | Overbank                 | $5.86 \pm 0.80$  | MAM    |
|                 | MB1     | 16-0115-002 | 1.7       | Terrace    | Overbank                 | $10.83 \pm 0.84$ | CAM    |
|                 | MB2     | 16-0115-003 | 1.4       | Floodplain | Overbank                 | $0.54 \pm 0.06$  | MAM    |
| Logan           | LOG1    | 16-0115-004 | 1.2       | Terrace    | Overbank                 | $8.88 \pm 0.81$  | CAM    |
|                 |         |             |           |            | Overbank                 | $7.51 \pm 0.82$  | MAM    |
|                 | LOG1    | 16-0115-005 | 1.6       | Terrace    | Overbank                 | $7.61 \pm 0.68$  | CAM    |
| Albert          | ALB     | 16-0115-007 | 1.1       | Terrace    | Overbank                 | $9.51 \pm 0.82$  | CAM    |
|                 | ALB     | 16-0115-008 | 1.5       | Terrace    | Overbank                 | $8.71 \pm 0.66$  | CAM    |
|                 | ALB     | 16-0115-009 | 1.9       | Terrace    | Overbank                 | $9.08 \pm 0.81$  | CAM    |
| Lockyer<br>[46] | LV1.1   | 14-0528-001 | 0.4       | Terrace    | Overbank                 | $11.51 \pm 1.29$ | CAM    |
|                 | LV1.2   | 14-0596-005 | 5.7       | Floodplain | Basal                    | $7.97 \pm 1.02$  | MAM    |
|                 | LV2.3   | 14-0596-015 | 0.2       | Terrace    | Overbank                 | $9.25 \pm 0.84$  | CAM    |
|                 | LV3.1   | 14-0596-001 | 0.4       | Terrace    | Overbank                 | $6.45 \pm 0.57$  | MAM    |
|                 | LV3.1   | 14-0528-010 | 2.1       | Terrace    | Overbank                 | $10.60 \pm 1.09$ | MAM    |
|                 | LV3.3   | 14-0528-008 | 9.4       | Floodplain | Basal                    | $7.34 \pm 0.67$  | MAM    |
|                 | LV3.8   | 14-0528-003 | 0.4       | Terrace    | Overbank                 | $9.50 \pm 0.93$  | CAM    |
|                 | LV4.3   | 14-0596-007 | 2.0       | Terrace    | Overbank                 | $10.01 \pm 1.23$ | MAM    |
|                 | LV4.4   | 14-0596-012 | 10.3      | Floodplain | Basal                    | $10.08 \pm 1.03$ | MAM    |

**Table 3.** Radiocarbon ages for the Logan River at Round Mountain.

| Basin | Core #/Depth (m) | Lab Code    | Material         | pMc   | $\delta^{13}C$ (‰) | Conventional Age (a BP) $\pm$ $1\sigma$ Error | 95.4% Calibrated Age (cal. BP) [%]                 |
|-------|------------------|-------------|------------------|-------|--------------------|-----------------------------------------------|----------------------------------------------------|
| Logan | LOG2/0.65        | BETA-482192 | Charred material | 97.18 | -24.3              | $230 \pm 30$                                  | 226–142 [67.8%]<br>306–252 [27.2%]<br>79–74 [0.4%] |
|       | LOG2/1.8         | BETA-482191 | Charred material | 93.5  | -25                | $540 \pm 30$                                  | 550–500                                            |

## 4. Discussion

### 4.1. Regional Correlation in Terrace Abandonment

Regional dating demonstrates that terraces ubiquitously bounded the macrochannels analyzed here. At all locations, valley fills were dominated by a terrace comprising 60–90% of the valley floor area. In most instances, these terrace surfaces were still inundated under the modern flow regime, but only by high-magnitude floods greater than a 20-year AEP (Figure 6). At all sites, the age determination of alluvium in the mid-reaches demonstrated an incisional episode between 7.5–10.8 ka (Figure 7), which was broadly synchronous with estimates of terrace abandonment in the mid-reaches of Lockyer Creek at  $9.6 \pm 0.98$  ka. Estimates of terrace abandonment throughout the region were all within  $1\sigma$  error and yielded a mean pooled age of  $9.24 \pm 0.93$  ka. Surficial ages of inset floodplains in two of the streams (Brisbane and Logan Rivers) suggested these units have been forming at least at timescales at  $10^2$ – $10^3$  years and were the locale of “active” flood deposition.

Contemporaneous early Holocene terrace abandonment was apparent in the regional correlation of terrace surface ages in north-eastern Australia (Figure 7). On the mid-north coast of New South Wales, early Holocene terrace abandonment was associated with laterally active river systems [18,21,22]. In the subtropical Fitzroy River basin, north of SEQ (Figure 2B), chronostratigraphic evidence indicates a peak in fluvial activity at 11 ka followed by a sharp decline through the remaining Holocene period [80]. However, the adjacent upper units of the terraces exhibited a mean pooled age of  $12.2 \pm 1.4$  ka [80]. These ages were obtained from samples 3–6 m below the surface and therefore probably underestimated the true age of terrace abandonment. As such, terrace abandonment in the Fitzroy River basin was likely to be younger than that presented in Figure 7 and may well be in the range presented for other subtropical streams. The comparative entrenched channel form (e.g.,

enlarged macrochannel that was constrained between the 10- and 100-year AEP floods) in this basin suggested a further regional phenomenon.

In the wet tropics (Figure 2B), nine OSL ages from terrace sediments and adjacent basal deposits in four basins suggest terraces were abandoned slightly earlier at  $10.3 \pm 1.3$  ka [23,24,81]. Basal OSL ages from the adjacent alluvial unit had a pooled mean age of  $7.5 \pm 0.9$  ka [81], which was similar to that investigated on the Lockyer. This was further indicative of a possible regional correlation with the subtropical rivers of SEQ. The fact that terrace abandonment ages in six of the seven basins presented in Figure 7 overlapped within  $1\sigma$  is a compelling argument for a regional climatic control and is discussed below.

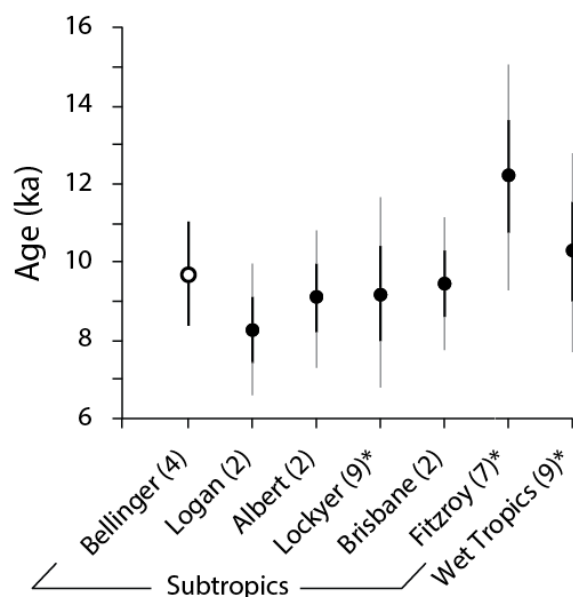


**Figure 7.** Mean terrace abandonment ages in north-eastern Australia. The number of samples per region is represented in brackets. Samples include OSL age determination from the upper terraces and, where noted by (\*), from basal samples in adjacent inset units. Fitzroy and wet tropics OSL ages after [24,80,81], respectively. Black bars represent  $1\sigma$  errors and grey bars represent  $2\sigma$  errors. The Bellinger basin age (hollow circle) was derived from conventional and AMS  $^{14}\text{C}$  ages [18,82], calibrated. Due to the differences in error calculations between OSL and  $^{14}\text{C}$  methods, errors for the Bellinger ages were the standard deviation of the population.

#### 4.2. Relationships to Late Quaternary Climatic Changes

The documented entrenchment/incision and the abandonment of previously active floodplains across SEQ closely aligned with widespread evidence of the onset of an early Holocene wet period in the subtropics and throughout eastern Australia between ca. 10–6 ka [26–28,37]. Channel incision during a glacial–interglacial transition is a commonly considered process in models of climatically-induced terrace development [83,84]. An increasingly warmer and wetter environment in SEQ may indeed have driven channel incision in the last glacial–interglacial transition and early Holocene [29,31]. Rapidly warming sea surface temperatures (SST) [85,86] may have presented a subtropical climate commensurate with the delivery of more extreme weather events [31].

Increased erosion in the wet tropics associated with the onset of wet conditions may have been more related to the strengthening of the summer monsoon [35,37,87,88]. Catchment instability, in the form of alluvial fan incision, slope instability, and changes to vegetation communities, were likely associated with higher humidity and rainfall events after 12 ka [88,89]. However, terrace abandonment ages within the wet tropics fall within  $1\sigma$  of those presented in this study (Figure 7) and may be indicative of climatic forcing throughout eastern Australia across the latitudinal range of 16–27° S, despite differences in climatic regimes.

Despite broad, regional differences in present climatic regimes, the proposed concept of a regional climatic factor could be observed in the modern regime. Within the present climate, dominated by multi-decadal wet and dry phases influenced by both ENSO [58] and the Interdecadal Pacific oscillation (IPO), there was generally a dominant spatial synchronicity of years with above average rainfall and flooding (Figure 8) [57]. In years where a strong La Niña had occurred, much of eastern Australia experienced very high anomalous rainfall and catastrophic flooding, as occurred in 1974 and 2011 (Figure 8). Such external climatic forcing may have also been reflected in the late Holocene riverine responses, with three of the four sites investigated in this study featuring pronounced flood deposits on adjacent surfaces dating to c. 0.5 ka (Figure 6).

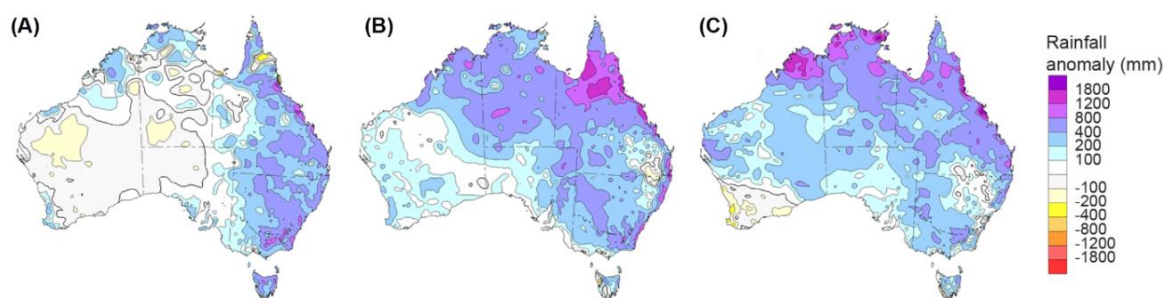


**Figure 8.** Maps of rainfall anomaly from long-term average conditions in Australia for water years September 1–August 31, (A) 1955, (B) 1974, and (C) 2011, demonstrating the tendency for broad continental trends in rainfall along the eastern margin. After [90].

#### 4.3. Alternative Drivers of Terrace Abandonment

The correlation of terrace abandonment provided an intriguing opportunity to explore the geomorphic controls on fluvial activity. If such terraces were driven by intrinsic factors [41], it is unlikely there would be basin-wide coherence in terrace formation, let alone across the sub-tropical region. However, the regional synchronicity of terrace abandonment and inset basal ages invoked an extrinsic control. Whilst a regional landscape response suggested a climate driver of channel incision in the Australian sub-tropics, it was important to evaluate alternatives.

While the minimal rates of uplift throughout the late Cenozoic [14] ruled out the role of tectonic processes, alternative interpretations of broad cut-and-fill episodes in SEQ could implicate eustatic base-level changes [91] or prehistoric human–landscape interactions [92]. Base-level changes over the late Quaternary would undoubtedly have had an impact to coastal rivers as sea-level transgression and regression of  $124 \pm 4$  m occurred along the eastern margin [93,94]. For such a control to be dominant on the timing of incision, as documented here, it would require a temporally consistent lag since lowstand-driven incision (assuming incision was initiated at, or prior to, the Last Glacial Maximum), was expressed across all basins. The incisional phase at  $9.24 \pm 0.93$  ka that formed the macrochannels in SEQ (Figure 7) occurred as the sea level rapidly rose from  $-30$  m below present mean sea level to  $+0.5$ – $1.5$  above modern at c.7 cal. ka BP [94]. As such, lowstand-driven incision could be discounted. This phase of incision counters an expected depositional response to sea-level changes [95,96]. The sites investigated in this study had elevations that ranged between 16–110 m and were above the inferred impacts of an immediate sea-level response [96].

Likewise, a changing environment throughout the late Quaternary most likely played a significant role in the population dynamics of Indigenous Australian people [97–99], who first inhabited the region  $>40$  ka [100,101]. Indigenous land management practices would have been spatially localized [98,102]. Although impacts may have occurred, it is challenging to decouple these from climate forcing at the broad landscape level and rationalize a ca. 30 ka lag in riverine response to human–landscape interactions. Without any sound evidence on the role of human impacts in the early Holocene and given the regional synchronicity in terrace abandonment ages and their association with other palaeoenvironmental records, we favor the role of a climatically-driven broad-scale fluvial response in

SEQ. What awaits further validation is the ultimate cause of this period of terrace formation, and the quantitative evidence for changes to runoff in this late Pleistocene/early Holocene period.

#### 4.4. Modern and Late Holocene Floodplain Dynamics

Following channel incision in the early Holocene, many streams in SEQ have been largely confined to their entrenched “macrochannel” form that remains preserved within the valley floor. While the macrochannels themselves may reflect a broadly similar entrenched morphology to arroyos in south-western United States [103,104], a lack of sediment supply limited the capacity for dynamic, cyclic responses commonly observed in arroyo valley fills [38,105]. As such, the modern floodplains in SEQ equated to narrow, depositional benches that formed within the macrochannel; in some cases, wider inset floodplains developed. The observed lack of a Holocene signal in the Fitzroy River basin may have been due to a lack of sediment preservation in a narrow (entrenched) fluvial corridor, or the dominance of in-channel bench formation [80]. Chronostratigraphic data of alluvial benches in Lockyer Creek indicated that these units had been the primary depositional sequences over the last 2000 years [78]. These inset units had been periodically stripped and reformed in relation to stochastic flood events and their formation may well be driven by intrinsic thresholds of channel capacity [41], relating to longitudinal distribution of flood power.

#### 4.5. Comparison to Terrace Abandonment in Other Climatic Regions

Invoking climate forcing in the formation of terraces is not a new or novel idea. Indeed, it is understood to be a principle driver of Cenozoic terrace formation globally [9,13,84,96]. Particularly, in regions affected by glacial ice sheets, global syntheses suggest the cyclicity of terrace staircases that reflect glacial-interglacial cycles [9,106]. Cold to warm transitions have produced coarse-grained deposits during glacial periods, with terraces capped by early-interglacial, vertically-accreting fines prior to abandonment [84]. This is a significant factor in glacially-fed fluvial systems, where melt water and changes to both flow regime and sediment supply were significant between glacial and interglacial cycles. Likewise, other regions may have experienced similar temperature-driven cyclicity in a fluvial response due to changes in vegetation cover and associated effects on sediment supply [106–108].

In humid climates, there is greater uncertainty as to the drivers of terrace formation and whether temperature or moisture flux had a more significant role (although these may be difficult to decouple). The important role of precipitation (aridity-humidity cycles influenced by global climate patterns) is seen as the dominant control on fluvial processes [109,110]. In these regions, humidity had a similar impact on ecological communities as temperature in cooler regions. In the wet tropics, moisture-driven changes in vegetation cover during the Last Glacial–Interglacial Transition initiated processes of landscape instability [88,111]. A shift between rainforest and dry sclerophyll forests critically impacted slope stability and sediment supply [89], although lowland terraces in the wet tropics did not appear to have been abandoned until the early Holocene (Figure 7). In contrast, empirical evidence from subtropical Australia suggests a positive moisture balance during the last Glacial period, with pollen from rainforest communities persisting in both the headwaters and lower reaches of the coastal-draining streams [31,112,113]. Indeed, the distribution of precipitation may have been a more important factor, particularly with regard to extreme events [114]. A precipitation maximum driven by changes in SST may have been significant enough to alter weather systems and increased the intensity of rainfall throughout the subtropical region during the early Holocene. As such, precipitation-driven terrace abandonment in the subtropics may have been associated with extreme events and may well have occurred rapidly. However, further research is required to evaluate exactly what elements of the environment the fluvial systems were responding to in the late Glacial to early Holocene.

Interestingly, entrenched channels with compound forms have also been identified in other regions noted for a lack of late Cenozoic uplift, such as the Indian subcontinent and the Kaapvaal Craton in South Africa [115]. While it is challenging to draw a comparison between the exact mechanisms of

terrace abandonment, particularly one of global climate forcing, crustal stability may be an important factor in the preservation of alluvial fills in such regions [9,115]. This tectonic stability may have ensured that terraces were abandoned slowly, had a polycyclic nature, and were retained in the landscape for extensive periods, exposing them to considerable weathering processes. Such factors would have increased the preservation potential of alluvial fills [116], and as such, allowed streams to retain entrenched channel forms over considerable periods, as with the macrochannels found in these regions [50,52].

## 5. Conclusions

This study presented a preliminary regional terrace chronology for subtropical SEQ, Australia. The results indicated a synchronous response of early Holocene channel incision and terrace abandonment that likely reflected large-scale climatic changes in eastern Australia. Chronostratigraphic interpretations from four basins within SEQ suggested a major phase of terrace abandonment between 7.5–10.8 ka with a mean age of  $9.24 \pm 0.93$  ka. This age range closely aligned with a precipitation maximum identified from other palaeoenvironmental records in eastern Australia. While intrinsic factors have likely impacted local scale variations in channel morphology, particularly within in-channel alluvial units, external climatic factors appear to have been the principal drivers of major phases of valley-scale erosion and deposition in subtropical Australia. The correlation with fluvial records elsewhere in the subtropics, and more broadly across eastern Australia, are further indication that terraces have been driven by climatic forcing. Further clarity around late Quaternary riverine responses within this region would be significantly enhanced by the addition of floodplain and palaeochannel chronologies and quantitative palaeodischarge calculations.

**Supplementary Materials:** The following are available online at <http://www.mdpi.com/2571-550X/1/3/23/s1>.

**Author Contributions:** Conceptualization, J.S.D. and T.J.C.; Methodology, J.S.D. and T.J.C.; Validation, J.S.D. and T.J.C.; Formal Analysis, J.S.D.; Investigation, J.S.D.; Data Curation, J.S.D.; Writing-Original Draft Preparation, J.S.D.; Writing-Review & Editing, J.S.D. and T.J.C.; Visualization, J.S.D.; Supervision, T.J.C.; Project Administration, J.S.D.

**Funding:** This research was funded in part by an Australian Research Council Linkage project, LP120200093, and industry partners DSITI, Seqwater, and Lockyer Valley Regional Council. Additional funding support was provided by a University of Queensland (UQ) Australian Postgraduate Award Scholarship.

**Acknowledgments:** The authors thank Jacky Croke as the LP project leader and Ashneel Sharma for his assistance with OSL analyses. We thank the journal editors and two anonymous reviewers for their comments and constructive input on this paper.

**Conflicts of Interest:** The authors declare no conflict of interest.

## References

1. Malatesta, L.C.; Prancevic, J.P.; Avouac, J.-P. Autogenic entrenchment patterns and terraces due to coupling with lateral erosion in incising alluvial channels. *J. Geophys. Res. Earth Surf.* **2017**, *122*, 335–355. [[CrossRef](#)]
2. Schumm, S.A. *The Fluvial System*; Wiley: New York, NY, USA, 1977.
3. Vandenberghe, J.; Cordier, S.; Bridgland, D.R. Extrinsic and intrinsic forcing of fluvial development: Understanding natural and anthropogenic influences. *Proc. Geol. Assoc.* **2010**, *121*, 107–112. [[CrossRef](#)]
4. Brierley, G.J.; Fryirs, K. *Geomorphology and River Management: Application of the Rivers Styles Framework*; Blackwell Publishing Ltd.: Malden, MA, USA, 2005.
5. Cooke, R.U.; Reeves, R.W. Arroyos and environmental change. *Oxford* **1976**, *328*, 520–557.
6. Dühnforth, M.; Anderson, R.S.; Ward, D.J.; Blum, A. Unsteady late pleistocene incision of streams bounding the colorado front range from measurements of meteoric and in situ  $^{10}\text{Be}$ . *J. Geophys. Res. Earth Surf.* **2012**, *117*. [[CrossRef](#)]
7. Malatesta, L.C.; Avouac, J.P.; Brown, N.D.; Breitenbach, S.F.M.; Pan, J.; Chevalier, M.L.; Rhodes, E.; Saint-Carlier, D.; Zhang, W.; Charreau, J.; et al. Lag and mixing during sediment transfer across the tian shan piedmont caused by climate-driven aggradation-incision cycles. *Basin Res.* **2017**. [[CrossRef](#)]

8. Maddy, D.; Bridgland, D.; Westaway, R. Uplift-driven incision and climate-controlled river terrace development in the Thames Valley, UK. *Quat. Int.* **2001**, *79*, 23–36. [[CrossRef](#)]
9. Bridgland, D.R.; Westaway, R. Climatically controlled river terrace staircases: A worldwide quaternary phenomenon. *Geomorphology* **2008**, *98*, 285–315. [[CrossRef](#)]
10. Hanson, P.R.; Mason, J.A.; Goble, R.J. Fluvial terrace formation along Wyoming's laramie range as a response to increased late pleistocene flood magnitudes. *Geomorphology* **2006**, *76*, 12–25. [[CrossRef](#)]
11. Macklin, M.G.; Lewin, J.; Jones, A.F. River entrenchment and terrace formation in the UK Holocene. *Quat. Sci. Rev.* **2013**, *76*, 194–206. [[CrossRef](#)]
12. Macklin, M.G.; Lewin, J.; Woodward, J.C. The fluvial record of climate change. *Philos. Trans. Ser. A Math. Phys. Eng. Sci.* **2012**, *370*, 2143–2172. [[CrossRef](#)] [[PubMed](#)]
13. Vandenberghe, J. The relation between climate and river processes, landforms and deposits. *Quat. Int.* **2002**, *91*, 17–23. [[CrossRef](#)]
14. Czarnota, K.; Roberts, G.G.; White, N.J.; Fishwick, S. Spatial and temporal patterns of Australian dynamic topography from river profile modeling. *J. Geophys. Res. Solid Earth* **2014**, *119*, 1384–1424. [[CrossRef](#)]
15. Nott, J.; Young, R.; McDougall, I. Wearing down, wearing back, and gorge extension in the long-term denudation of a highland mass: Quantitative evidence from the Shoalhaven catchment, Southeast Australia. *J. Geol.* **1996**, *104*, 224–232. [[CrossRef](#)]
16. Peel, M.C.; McMahon, T.A.; Finlayson, B.L. Continental differences in the variability of annual runoff—update and reassessment. *J. Hydrol.* **2004**, *295*, 185–197. [[CrossRef](#)]
17. Rustomji, P.; Bennett, N.; Chiew, F. Flood variability east of Australia's great dividing range. *J. Hydrol.* **2009**, *374*, 196–208. [[CrossRef](#)]
18. Cohen, T.J.; Nanson, G.C. Topographically associated but chronologically disjunct late quaternary floodplains and terraces in a partly confined valley, south-eastern Australia. *Earth Surf. Process. Landf.* **2008**, *33*, 424–443. [[CrossRef](#)]
19. Kermode, S.J.; Cohen, T.J.; Reinfelds, I.V.; Nanson, G.C.; Pietsch, T.J. Alluvium of antiquity: Polycyclic terraces in a confined bedrock valley. *Geomorphology* **2012**, *139–140*, 471–483. [[CrossRef](#)]
20. Cheetham, M.D.; Keene, A.F.; Erskine, W.D.; Bush, R.T.; Fitzsimmons, K.; Jacobsen, G.E.; Fallon, S.J. Resolving the Holocene alluvial record in southeastern Australia using luminescence and radiocarbon techniques. *J. Quat. Sci.* **2010**, *25*, 1160–1168. [[CrossRef](#)]
21. Nanson, G.C.; Cohen, T.J.; Doyle, C.J.; Price, D.M. Alluvial evidence of major late-quaternary climate and flow-regime changes on the coastal rivers of New South Wales, Australia. In *Palaeohydrology: Understanding Global Change*; Gregory, K.J., Benito, G., Eds.; John Wiley & Sons, Ltd.: Chichester, UK, 2003; pp. 233–258.
22. Cohen, T.J.; Nanson, G.C. Mind the gap: An absence of valley-fill deposits identifying the Holocene hypsithermal period of enhanced flow regime in southeastern Australia. *Holocene* **2007**, *17*, 411–418. [[CrossRef](#)]
23. Hughes, K.; Croke, J.C.; Bartley, R.; Thompson, C.J.; Sharma, A. Alluvial terrace preservation in the wet tropics, northeast Queensland, Australia. *Geomorphology* **2015**, *248*, 311–326. [[CrossRef](#)]
24. Leonard, S.; Nott, J. Rapid cycles of episodic adjustment: Understanding the Holocene fluvial archive of the Daintree River of northeastern Australia. *Holocene* **2015**, *25*, 1208–1219. [[CrossRef](#)]
25. Nott, J.; Hayne, M. High frequency of 'super-cyclones' along the Great Barrier Reef over the past 5000 years. *Nature* **2001**, *413*, 508–512. [[CrossRef](#)] [[PubMed](#)]
26. Kershaw, A.P. Environmental change in Greater Australia. *Antiquity* **1995**, *69*, 656–675. [[CrossRef](#)]
27. Kershaw, A.P.; D'Costa, D.M.; McEwen Mason, J.R.C.; Wagstaff, B.E. Palynological evidence for quaternary vegetation and environments of mainland Southeastern Australia. *Quat. Sci. Rev.* **1991**, *10*, 391–404. [[CrossRef](#)]
28. Petherick, L.; Bostock, H.; Cohen, T.J.; Fitzsimmons, K.; Tibby, J.; Fletcher, M.S.S.; Moss, P.; Reeves, J.; Mooney, S.; Barrows, T.; et al. Climatic records over the past 30ka from temperate Australia—A synthesis from the Oz-Intimate workgroup. *Quat. Sci. Rev.* **2013**, *74*, 58–77. [[CrossRef](#)]
29. Reeves, J.M.; Barrows, T.T.; Cohen, T.J.; Kiem, A.S.; Bostock, H.C.; Fitzsimmons, K.E.; Jansen, J.D.; Kemp, J.; Krause, C.; Petherick, L.; et al. Climate variability over the last 35,000 years recorded in marine and terrestrial archives in the Australian region: An Oz-Intimate compilation. *Quat. Sci. Rev.* **2013**, *74*, 21–34. [[CrossRef](#)]
30. Kershaw, A.P.; McKenzie, G.M.; Porch, N.; Roberts, R.G.; Brown, J.; Heijnis, H.; Orr, M.L.; Jacobsen, G.; Newall, P.R. A high-resolution record of vegetation and climate through the last glacial cycle from Caledonia Fen, Southeastern Highlands of Australia. *J. Quat. Sci.* **2007**, *22*, 481–500. [[CrossRef](#)]



31. Moss, P.T.; Tibby, J.; Petherick, L.; McGowan, H.A.; Barr, C. Late quaternary vegetation history of North Stradbroke Island, Queensland, Eastern Australia. *Quat. Sci. Rev.* **2013**, *74*, 257–272. [[CrossRef](#)]
32. Turney, C.S.M.; Kershaw, A.P.; Clemens, S.C.; Branch, N.; Moss, P.T.; Fifield, L.K. Millennial and orbital variations of el niño/southern oscillation and high-latitude climate in the last glacial period. *Nature* **2004**, *428*, 306–310. [[CrossRef](#)] [[PubMed](#)]
33. Jones, R.; Bowler, J.; McMahon, T. A high resolution holocene record of p/e ratio from Closed Lakes, Western Victoria. *Palaeoclimates* **1998**, *3*, 51–82.
34. Wilkins, D.; Gouramanis, C.; De Deckker, P.; Fifield, L.K.; Olley, J. Holocene lake-level fluctuations in Lakes Keilambete and Gnotuk, Southwestern Victoria, Australia. *Holocene* **2013**, *23*, 784–795. [[CrossRef](#)]
35. Wyrwoll, K.-H.H.; Miller, G.H. Initiation of the Australian summer monsoon 14,000 years ago. *Quat. Int.* **2001**, *83–85*, 119–128. [[CrossRef](#)]
36. Woodward, C.; Shulmeister, J.; Bell, D.; Haworth, R.; Jacobsen, G.; Zawadzki, A. A holocene record of climate and hydrological changes from Little Llangothlin Lagoon, South Eastern Australia. *Holocene* **2014**, *24*, 1–10. [[CrossRef](#)]
37. Reeves, J.M.; Bostock, H.C.; Ayliffe, L.K.; Barrows, T.T.; De Deckker, P.; Devriendt, L.S.; Dunbar, G.B.; Drysdale, R.N.; Fitzsimmons, K.E.; Gagan, M.K.; et al. Palaeoenvironmental change in tropical Australasia over the last 30,000 years—A synthesis by the Oz-Intimate group. *Quat. Sci. Rev.* **2013**, *74*, 97–114. [[CrossRef](#)]
38. Harvey, J.E.; Pederson, J.L.; Rittenour, T.M. Exploring relations between arroyo cycles and canyon paleoflood records in buckskin wash, Utah: Reconciling scientific paradigms. *Bull. Geol. Soc. Am.* **2011**, *123*, 2266–2276. [[CrossRef](#)]
39. Erskine, W.D.; Livingstone, E.A. In-channel benches: The role of floods in their formation and destruction on bedrock-confined rivers. In *Varieties of Fluvial Form*; Miller, A.J., Gupta, A., Eds.; John Wiley & Sons, Ltd.: Chichester, UK, 1999; pp. 445–476.
40. Nanson, G.C. Episodes of vertical accretion and catastrophic stripping: A model of disequilibrium flood-plain development. *Geol. Soc. Am. Bull.* **1986**, *97*, 1467–1475. [[CrossRef](#)]
41. Thompson, C.J.; Croke, J.C.; Fryirs, K.; Grove, J.R. A channel evolution model for subtropical macrochannel systems. *CATENA* **2016**, *139*, 199–213. [[CrossRef](#)]
42. Erskine, W.D.; Saynor, M. Effects of catastrophic floods on sediment yields in Southeastern Australia. In *Erosion and Sediment Yield: Global and Regional Perspectives, Proceedings of the International Symposium, Exeter, UK, 15–19 July 1996*; IAHS: London, UK; p. 381.
43. Baker, V.R. Stream-channel responses to floods, with examples from central Texas. *Geol. Soc. Am. Bull.* **1977**, *88*, 1057–1071. [[CrossRef](#)]
44. Croke, J.C.; Fryirs, K.; Thompson, C.J. Channel-floodplain connectivity during an extreme flood event: Implications for sediment erosion, deposition, and delivery. *Earth Surf. Process. Landf.* **2013**, *38*, 1444–1456. [[CrossRef](#)]
45. Croke, J.C.; Reinfelds, I.; Thompson, C.J.; Roper, E. Macrochannels and their significance for flood-risk minimisation: Examples from Southeast Queensland and New South Wales, Australia. *Stoch. Environ. Res. Risk Assess.* **2014**, *28*, 99–112. [[CrossRef](#)]
46. Daley, J.S.; Croke, J.; Thompson, C.; Cohen, T.; Macklin, M.; Sharma, A. Late quaternary channel and floodplain formation in a partly confined Subtropical River, Eastern Australia. *J. Quat. Sci.* **2017**, *32*, 729–743. [[CrossRef](#)]
47. Grove, J.R.; Croke, J.C.; Thompson, C.J. Quantifying different riverbank erosion processes during an extreme flood event. *Earth Surf. Process. Landf.* **2013**. [[CrossRef](#)]
48. Thompson, C.J.; Croke, J.C. Geomorphic effects, flood power, and channel competence of a catastrophic flood in confined and unconfined reaches of the Upper Lockyer Valley, Southeast Queensland, Australia. *Geomorphology* **2013**, *197*, 156–169. [[CrossRef](#)]
49. Croke, J.C.; Todd, P.; Thompson, C.J.; Watson, F.; Denham, R.; Khanal, G. The use of multi temporal lidar to assess basin-scale erosion and deposition following the catastrophic January 2011 Lockyer Flood, SE Queensland, Australia. *Geomorphology* **2013**, *184*, 111–126. [[CrossRef](#)]
50. Heritage, G.L.L.; Broadhurst, L.J.J.; Birkhead, A.L.L. The influence of contemporary flow regime on the geomorphology of the Sabie River, South Africa. *Geomorphology* **2001**, *38*, 197–211. [[CrossRef](#)]
51. Van Niekerk, A.W.; Heritage, G.L.; Broadhurst, L.J.; Moon, B.P. Bedrock anastomosing channel systems: Morphology and dynamics in the Sabie River, Mpumalanga Province, South Africa. In *Varieties of Fluvial Form*; Miller, A.J., Gupta, A., Eds.; John Wiley & Sons, Ltd.: Chichester, UK, 1999; pp. 33–52.

52. Gupta, A. Magnitude, frequency, and special factors affecting channel form and processes in the seasonal tropics. In *Natural and Anthropogenic Influences in Fluvial Geomorphology*; Costa, J.E., Miller, A.J., Potter, K.W., Wilcock, P.R., Eds.; American Geophysical Union: Washington, DC, USA, 1995; pp. 125–136.
53. Hoyle, J.; Brooks, A.P.; Brierley, G.J.; Fryirs, K.; Lander, J. Spatial variability in the timing, nature and extent of channel response to typical human disturbance along the Upper Hunter River, New South Wales, Australia. *Earth Surf. Process. Landf.* **2008**, *33*, 868–889. [[CrossRef](#)]
54. Woodyer, K.D.D. Bankfull frequency in rivers. *J. Hydrol.* **1968**, *6*, 114–142. [[CrossRef](#)]
55. Harden, T.; Macklin, M.G.; Baker, V.R. Holocene flood histories in South-Western USA. *Earth Surf. Process. Landf.* **2010**, *35*, 707–716. [[CrossRef](#)]
56. Crimp, S.J.; Day, K.A. Evaluation of multi-decadal variability in rainfall in queensland using indices of el nino-southern oscillation and inter-decadal variability. In *Science for Drought, Proceedings of the National Drought Forum*; Stone, R.C., Partridge, I., Eds.; National Drought Forum: Brisbane, Australia, 2003; pp. 106–115.
57. Kiem, A.S. Multi-decadal variability of flood risk. *Geophys. Res. Lett.* **2003**, *30*, 1035–1035. [[CrossRef](#)]
58. Power, S.; Casey, T.; Folland, C.; Colman, A.; Mehta, V. Inter-decadal modulation of the impact of enso on australia. *Clim. Dyn.* **1999**, *15*, 319–324. [[CrossRef](#)]
59. Risbey, J.; Karoly, D.; Reynolds, A.; Braganza, K. Drought and climate change. In *Proceedings of the National Drought Forum, Brisbane, Australia, 15–16 April 2003*; Stone, R.C., Partridge, I., Eds.; National Drought Forum: Brisbane, Australia, 2003; pp. 8–11.
60. Daley, J.S. *Late Quaternary Stream Channel Adjustment in Hydrologically Variable Catchments, Subtropical Australia*; University of Queensland: Brisbane, Australia, 2018.
61. Pasternack, G.B. *Lower Yuba River Corridor Inundation Zones. Prepared for The Yuba County Water Agency*; University of California: Davis, CA, USA, 2017.
62. Weber, M.D.; Pasternack, G.B. *2014 Topographic Mapping of the Lower Yuba River. Prepared for the Yuba Accord River Management Team*; University of California: Davis, CA, USA, 2016.
63. Aitken, M.J. *An Introduction to Optical Dating: The Dating of Quaternary Sediments by the Use of Photon-Stimulated Luminescence*; Oxford Science Publications: Oxford, UK, 1998.
64. Wallinga, J. Optically stimulated luminescence dating of fluvial deposits: A review. *Boreas* **2002**, *31*, 303–322. [[CrossRef](#)]
65. Olley, J.M.; Pietsch, T.J.; Roberts, R.G. Optical dating of holocene sediments from a variety of geomorphic settings using single grains of quartz. *Geomorphology* **2004**, *60*, 337–358. [[CrossRef](#)]
66. Pietsch, T.J. Optically stimulated luminescence dating of young (<500 years old) sediments: Testing estimates of burial dose. *Quat. Geochronol.* **2009**, *4*, 406–422.
67. Galbraith, R.F. Graphical display of estimates having differing standard errors. *Technometrics* **1988**, *30*, 271–281. [[CrossRef](#)]
68. Galbraith, R.F.; Laslett, G.M. Statistical models for mixed fission track ages. *Nucl. Tracks Radiat. Meas.* **1993**, *21*, 459–470. [[CrossRef](#)]
69. Galbraith, R.F.; Roberts, R.G.; Laslett, G.M.; Yoshida, H.; Olley, J.M. Optical dating of single and multiple grains of quartz from Jinmium Rock Shelter, Northern Australia, part 2, results and implications. *Archaeometry* **1999**, *41*, 339–364. [[CrossRef](#)]
70. Roberts, H.M.; Wintle, A.G. Equivalent dose determinations for polymineralic fine-grains using the sar protocol: Application to a holocene sequence of the chinese loess plateau. *Quat. Sci. Rev.* **2001**, *20*, 859–863. [[CrossRef](#)]
71. Murray, A.; Marten, R.; Johnston, A.; Martin, P. Analysis for naturally occurring radionuclides at environmental concentrations by gamma spectrometry. *J. Radioanal. Nucl. Chem.* **1987**, *115*, 263–288. [[CrossRef](#)]
72. Stokes, S.; Ingram, S.; Aitken, M.J.; Sirocko, F.; Anderson, R.; Leuschner, D. Alternative chronologies for late quaternary (last interglacial–holocene) deep sea sediments via optical dating of silt-sized quartz. *Quat. Sci. Rev.* **2003**, *22*, 925–941. [[CrossRef](#)]
73. Mejdahl, V. Thermoluminescence dating: Beta-dose attenuation in quartz grains. *Archaeometry* **1979**, *21*, 61–72. [[CrossRef](#)]
74. Prescott, J.R.; Hutton, J.T. Cosmic ray contributions to dose rates for luminescence and ESR dating: Large depths and long-term time variations. *Radiat. Meas.* **1994**, *23*, 497–500. [[CrossRef](#)]

75. Bowler, J.M.; Johnston, H.; Olley, J.M.; Prescott, J.R.; Roberts, R.G.; Shawcross, W.; Spooner, N.A. New ages for human occupation and climatic change at Lake Mungo, Australia. *Nature* **2003**, *421*, 837–840. [[CrossRef](#)] [[PubMed](#)]
76. Stuiver, M.; Polach, H.A. Discussion; reporting of c-14 data. *Radiocarbon* **1977**, *19*, 355–363. [[CrossRef](#)]
77. Reimer, P.J.; Bard, E.; Bayliss, A.; Beck, J.W.; Blackwell, P.G.; Bronk Ramsey, C.; Buck, C.E.; Cheng, H.; Edwards, R.L.; Friedrich, M.; et al. Intcal13 and marine13 radiocarbon age calibration curves 0–50,000 years cal BP. *Radiocarbon* **2013**, *55*, 1869–1887. [[CrossRef](#)]
78. Croke, J.; Thompson, C.; Denham, R.; Haines, H.; Sharma, A.; Pietsch, T. Reconstructing a millennial-scale record of flooding in a single valley setting: The 2011 flood-affected Lockyer Valley, South-East Queensland, Australia. *J. Quat. Sci.* **2016**, *31*, e2919. [[CrossRef](#)]
79. Kermodé, S.J.; Cohen, T.J.; Reinfelds, I.V.; Jones, B.G. Modern depositional processes in a confined, flood-prone setting: Benches on the Shoalhaven River, NSW, Australia. *Geomorphology* **2015**, *228*, 470–485. [[CrossRef](#)]
80. Croke, J.C.; Jansen, J.D.; Amos, K.; Pietsch, T.J. A 100 ka record of fluvial activity in the Fitzroy River Basin, Tropical Northeastern Australia. *Quat. Sci. Rev.* **2011**, *30*, 1681–1695. [[CrossRef](#)]
81. Hughes, K.; Croke, J.C. How did rivers in the wet tropics (Ne Queensland, Australia) respond to climate changes over the past 30 000 years? *J. Quat. Sci.* **2017**, *32*, 744–759. [[CrossRef](#)]
82. Warner, R.F. Radio-carbon dates for some fluvial and colluvial deposits in the Bellinger Valleys, New South Wales. *Aust. J. Sci.* **1970**, *32*, 368–369.
83. Gibbard, P.L.; Lewin, J. River incision and terrace formation in the Late Cenozoic of Europe. *Tectonophysics* **2009**, *474*, 41–55. [[CrossRef](#)]
84. Vandenberghe, J. River terraces as a response to climatic forcing: Formation processes, sedimentary characteristics and sites for human occupation. *Quat. Int.* **2015**, *370*, 3–11. [[CrossRef](#)]
85. Chang, J.C.; Shulmeister, J.; Woodward, C.; Steinberger, L.; Tibby, J.; Barr, C. A chironomid-inferred summer temperature reconstruction from subtropical Australia during the last glacial maximum (LGM) and the last deglaciation. *Quat. Sci. Rev.* **2015**, *122*, 282–292. [[CrossRef](#)]
86. Woltering, M.; Atahan, P.; Grice, K.; Heijnis, H.; Taffs, K.; Dodson, J. Glacial and holocene terrestrial temperature variability in subtropical east Australia as inferred from branched gdt distributions in a sediment core from lake mckenzie. *Quat. Res.* **2014**, *82*, 132–145. [[CrossRef](#)]
87. Field, E.; Tyler, J.; Gadd, P.S.; Moss, P.; McGowan, H.; Marx, S. Coherent patterns of environmental change at multiple organic spring sites in northwest Australia: Evidence of Indonesian-Australian summer monsoon variability over the last 14,500 years. *Quat. Sci. Rev.* **2018**, *196*, 193–216. [[CrossRef](#)]
88. Thomas, M.F. Understanding the impacts of late quaternary climate change in tropical and sub-tropical regions. *Geomorphology* **2008**, *101*, 146–158. [[CrossRef](#)]
89. Thomas, M.F.; Nott, J.; Murray, A.S.; Price, D.M. Fluvial response to late quaternary climate change in Ne Queensland, Australia. *Palaeogeogr. Palaeoclim. Palaeoecol.* **2007**, *251*, 119–136. [[CrossRef](#)]
90. Bureau of Meteorology. *Rainfall Anomalies (mm)—Product of the National Climate Centre*; Australian Government, Bureau of Meteorology: Melbourne, Australia, 2012.
91. Beckmann, G.G. *The Post-Tertiary History of Brisbane And Surroundings*; University of Queensland: Brisbane, Australia, 1959.
92. Bowman, D.M.J.S. The impact of aboriginal landscape burning on the Australian biota. *New Phytol.* **1998**, *140*, 385–410. [[CrossRef](#)]
93. Chivas, A.R.; García, A.; van der Kaars, S.; Couapel, M.J.J.; Holt, S.; Reeves, J.M.; Wheeler, D.J.; Switzer, A.D.; Murray-Wallace, C.V.; Banerjee, D.; et al. Sea-level and environmental changes since the last interglacial in the Gulf of Carpentaria, Australia: An overview. *Quat. Int.* **2001**, *83–85*, 19–46. [[CrossRef](#)]
94. Lewis, S.E.; Sloss, C.R.; Murray-Wallace, C.V.; Woodroffe, C.D.; Smithers, S.G. Post-glacial sea-level changes around the Australian margin: A review. *Quat. Sci. Rev.* **2013**, *74*, 115–138. [[CrossRef](#)]
95. Blum, M.D.; Aslan, A. Signatures of climate vs. Sea-level change within incised valley-fill successions: Quaternary examples from the Texas Gulf coast. *Sediment. Geol.* **2006**, *190*, 177–211. [[CrossRef](#)]
96. Blum, M.D.; Törnqvist, T.E. Fluvial responses to climate and sea-level change: A review and look forward. *J. Int. Assoc. Sedimentol.* **2000**, *47*, 2–48. [[CrossRef](#)]
97. Turney, C.S.M.; Hobbs, D. ENSO influence on Holocene Aboriginal populations in Queensland, Australia. *J. Archaeol. Sci.* **2006**, *33*, 1744–1748. [[CrossRef](#)]

98. Williams, A.N.; Mooney, S.D.; Sisson, S.A.; Marlon, J. Exploring the relationship between aboriginal population indices and fire in Australia over the last 20,000 years. *Palaeogeogr. Palaeoclim. Palaeoecol.* **2015**, *432*, 49–57. [[CrossRef](#)]
99. Williams, A.N.; Ulm, S.; Goodwin, I.D.; Smith, M. Hunter-gatherer response to late holocene climatic variability in Northern and Central Australia. *J. Quat. Sci.* **2010**, *25*, 831–838. [[CrossRef](#)]
100. Allen, J.; O'Connell, J. Both half right: Updating the evidence for dating first human arrivals in Sahul. *Aust. Archaeol.* **2014**, *79*, 86–108. [[CrossRef](#)]
101. Neal, R.; Stock, E. Pleistocene occupation in the South-East Queensland Coastal Region. *Nature* **1986**, *323*, 618. [[CrossRef](#)]
102. Bird, R.B.; Bird, D.W.; Coddling, B.F.; Parker, C.H.; Jones, J.H. The “fire stick farming” hypothesis: Australian aboriginal foraging strategies, biodiversity, and anthropogenic fire mosaics. *Proc. Natl. Acad. Sci. USA* **2008**, *105*, 14796–14801. [[CrossRef](#)] [[PubMed](#)]
103. Bull, W.B. Discontinuous ephemeral streams. *Geomorphology* **1997**, *19*, 227–276. [[CrossRef](#)]
104. Elliott, J.G.; Gellis, A.C.; Aby, S.B. Evolution of arroyos: Incised channels of the southwestern United States. In *Incised River Channels: Processes, Forms, Engineering and Management*; Darby, S.E., Simon, A., Eds.; Wiley: Chichester, UK, 1999; pp. 153–186.
105. Waters, M.R. Alluvial chronologies and archaeology of the Gila River Drainage Basin, Arizona. *Geomorphology* **2008**, *101*, 332–341. [[CrossRef](#)]
106. Macklin, M.G.; Fuller, I.C.; Lewin, J.; Maas, G.S.; Passmore, D.G.; Rose, J.; Woodward, J.C.; Black, S.; Hamlin, R.H.B.; Rowan, J.S. Correlation of fluvial sequences in the Mediterranean basin over the last 200 ka and their relationship to climate change. *Quat. Sci. Rev.* **2002**, *21*, 1633–1641. [[CrossRef](#)]
107. Macklin, M.G.; Lewin, J. Alluvial responses to the changing earth system. *Earth Surf. Process. Landf.* **2008**, *33*, 1374–1395. [[CrossRef](#)]
108. Doğan, U. Fluvial response to climate change during and after the last glacial maximum in Central Anatolia, Turkey. *Quat. Int.* **2010**, *222*, 221–229. [[CrossRef](#)]
109. Jain, M.; Tandon, S.K. Fluvial response to late quaternary climate changes, Western India. *Quat. Sci. Rev.* **2003**, *22*, 2223–2235. [[CrossRef](#)]
110. Latrubesse, E.M.; Bocquentin, J.; Santos, J.C.R.; Ramonell, C.G. Paleoenvironmental model for the late Cenozoic of southwestern Amazonia: Paleontology and geology. *Acta Amazon.* **1997**, *27*, 103–117. [[CrossRef](#)]
111. Kershaw, A.P. Climatic change and aboriginal burning in North-East Australia during the last two glacial/interglacial cycles. *Nature* **1986**, *322*, 47. [[CrossRef](#)]
112. Ellerton, D.; Shulmeister, J.; Woodward, C.; Moss, P. Last glacial maximum and last glacial–interglacial transition pollen record from Northern NSW, Australia: Evidence for a humid late last glacial maximum and dry deglaciation in parts of Eastern Australia. *J. Quat. Sci.* **2017**, *32*, 717–728. [[CrossRef](#)]
113. Petherick, L.M.; Moss, P.T.; McGowan, H.A. An extended last glacial maximum in Subtropical Australia. *Quat. Int.* **2016**, *432*, 1–12. [[CrossRef](#)]
114. Vandenberghe, J. Climate forcing of fluvial system development: An evolution of ideas. *Quat. Sci. Rev.* **2003**, *22*, 2053–2060. [[CrossRef](#)]
115. Westaway, R.; Bridgland, D.; Mishra, S. Rheological differences between archaean and younger crust can determine rates of quaternary vertical motions revealed by fluvial geomorphology. *Terra Nova* **2003**, *15*, 287–298. [[CrossRef](#)]
116. Lewin, J.; Macklin, M.G. Preservation potential for late quaternary river alluvium. *J. Quat. Sci.* **2003**, *18*, 107–120. [[CrossRef](#)]

